Combined First-Principles Computational and Experimental Multinuclear Solid-State NMR Investigation of Amino Acids

Christel Gervais,*,† Ray Dupree,‡ Kevin J. Pike,‡ Christian Bonhomme,† Mickaël Profeta,§ Chris J. Pickard,|| and Francesco Mauri§

Laboratoire de Chimie de la Matière Condensée - UMR CNRS 7574 - Université Pierre et Marie Curie, 4 place Jussieu, 75005 Paris, France, Department of Physics, University of Warwick, Coventry, CV4 7AL, United Kingdom, Laboratoire de Minéralogie-Cristallographie de Paris - UMR CNRS 7590 - Université Pierre et Marie Curie, 4 place Jussieu, 75005 Paris, France, TCM Group, Cavendish Laboratory, Madingley Road, Cambridge CB3 OHE, United Kingdom

Received: March 17, 2005; In Final Form: June 9, 2005

^{13}C, ^{14}N, ^{15}N, ^{17}O, and ^{35}Cl NMR parameters, including chemical shift tensors and quadrupolar tensors for ^{14}N,^{17}O, and ^{35}Cl, are calculated for the crystalline forms of various amino acids under periodic boundary conditions and complemented by experiment where necessary. The ^{13}C shift tensors and ^{14}N electric field gradient (EFG) tensors are in excellent agreement with experiment. Similarly, static ^{17}O NMR spectra could be precisely simulated using the calculation of the full chemical shift (CS) tensors and their relative orientation with the EFG tensors. This study allows correlations to be found between hydrogen bonding in the crystal structures and the ^{17}O NMR shielding parameters and the ^{35}Cl quadrupolar parameters, respectively. Calculations using the two experimental structures for L-alanine have shown that, while the calculated isotropic chemical shift values of ^{13}C and ^{15}N are relatively insensitive to small differences in the experimental structure, the ^{17}O shift is markedly affected.

Introduction

A key experimental challenge for biomolecular chemistry is to provide detailed information about the molecular bonding arrangement and changes that occur upon ligand−receptor interaction. Solid-state NMR is one nonperturbing approach which can be used to study such interactions, since chemical shift and quadrupolar coupling constants are known to be excellent probes for molecular conformation and intermolecular interactions.

^{17}O is a particularly powerful probe, since its chemical shift range covers almost 1000 ppm in organic molecules, compared with ∼250 ppm for ^{13}C, and it has a quadrupole moment ($I = {}^5/_2$) so that the electric field gradient (EFG), which is very sensitive to the molecular geometry of the investigated site, strongly affects the solid-state NMR spectrum. Recently, the experimental determination of ^{17}O NMR tensors was reported by Wu et al. in crystalline amides,[1] nucleic acid bases,[2] and potassium hydrogen dibenzoate,[3] and the EFG and isotropic shifts in glutamates[4] and amino acids by Pike et al.[5] It appears that reliable solid-state ^{17}O NMR magic-angle spinning (MAS) and static spectra can be obtained at relatively high field on ^{17}O-enriched compounds and that ^{17}O NMR tensors are highly sensitive to the local intermolecular hydrogen-bonding interactions.

Only a few ^{35}Cl solid-state NMR studies, mostly of inorganic materials, have been reported to date. Chloride salts with cubic symmetry exhibit very small C_Q values and could therefore be investigated by slow MAS.[6,7] Similarly, perchlorate derivatives showing small C_Q values, because of the tetrahedral symmetry of the anions, have been studied at high field under MAS.[8] In contrast, ^{35}Cl for covalently bonded chlorine in organic compounds typically shows very large quadrupolar interactions[9] ($20 \leq C_Q \leq 80$ MHz) and has only been observed by nuclear quadrupole resonance (NQR). Interestingly, intermediate C_Q values are observed for chloride anions involved in some inorganic or organic structures. For chlorinated Al−O−P clusters, C_Q values ranging from 5.8 to 7.8 MHz were observed,[10] while for *n*-decylammonium chloride,[11] tris(sarcosine)calcium chloride,[12] and cocaine hydrochloride,[13] the C_Q values are 2.43, 4.30, and 5.02 MHz, respectively. A recent study used several solid-state NMR techniques at 9.4 and 18.8 T to examine both ^{35}Cl and ^{37}Cl in some organic hydrochlorides, among which were L-tyrosine−HCl.[14] In all these cases, the role of N−H····Cl hydrogen bonds is emphasized.

Traditional quantum chemistry codes are able to calculate NMR shielding parameters for isolated systems, and first-principles quantum-mechanical cluster calculations of shielding parameters have proven to be a useful tool in assigning experimental ^{17}O and ^{35}Cl NMR spectra in small biological molecules.[2,14] To calculate NMR parameters for an extended system, such as a molecular crystal, it is necessary to construct a cluster of molecules such that the site of interest has the same local environment as in the full crystal. The main objectives of this study are to evaluate the quality of first-principles calculations to determine the full ^{13}C, ^{14}N, ^{15}N, ^{17}O, and ^{35}Cl chemical shift (CS) and EFG (for quadrupolar nuclei) tensors as well as

† Laboratoire de Chimie de la Matière Condensée.
‡ University of Warwick.
§ Laboratoire de Minéralogie-Cristallographie de Paris.
|| Cavendish Laboratory.

10.1021/jp0513925 CCC: $30.25
Published on Web 07/19/2005

their relative orientations in biomolecular solids and to try to determine possible correlations between these NMR parameters and intermolecular bonding Calculations use a recently developed method[15] based on density functional theory (DFT) and the plane-wave pseudopotential approach, which allows the calculation of NMR parameters in periodic systems. This method has already given very satisfactory results for the isotropic shifts in glutamic acid polymorphs.[16] As these calculations are based on the full crystal structures rather than a cluster, they provide a direct link between the structural features and the NMR parameters. Note that the NMR parameters of all the nuclei present are determined simultaneously.

Calculations are particularly useful for quadrupolar nuclei, because the combination of chemical shift and EFG makes line assignment more certain, and because it is difficult to determine the full tensors by analyzing static NMR spectra (five unknowns plus three angles), particularly if more than one site is present. In addition, calculations can provide the absolute orientation of the EFG and CS tensors in the molecular frame. This paper details the results of the complete NMR first-principles calculations of various amino acids complemented by the corresponding experimental solid-state NMR study where necessary. Experimental ^{17}O isotropic chemical shifts and EFG parameters in these samples have recently been reported,[5] but ^{17}O static spectra and their simulations, including the full CS tensors and their relative orientation with the EFG tensors, as well as experimental ^{35}Cl spectra, are additionally presented here. This study allows correlations to be found between ^{17}O NMR shielding parameters or ^{35}Cl quadrupolar parameters and hydrogen bonding in the crystal structures.

Experimental Section

The ^{17}O-enriched amino acids were those used by Pike et al.[5] Typical enrichment was 10−20%. Most of the NMR experiments were carried out on a Chemagnetics Infinity 600 spectrometer at a frequency of 81.345 MHz for ^{17}O and 58.80 MHz for ^{35}Cl with some additional ^{17}O static spectra being acquired at a magnetic field of 8.45 T and a frequency of 48.8 MHz. The MAS experiments used a 4 mm probe spinning at ∼16 kHz. A spin−echo was used with the echo spacing set to the rotation period. Static experiments were carried out in the same probe with a similar (∼65 μs) echo spacing. Typical pulse lengths were 0.9 μs and 1.8 μs for ^{17}O and 1.2 μs and 2.4 μs for ^{35}Cl. The recycle delay for ^{17}O was typically 2 s, and it was 0.5 s for ^{35}Cl. The ^{17}O spectra were referenced to water at 0 ppm and ^{35}Cl to solid NaCl taken as 0 ppm.

The shapes of the ^{17}O static spectra were simulated using the *SIMPSON* program[17] using the theoretically calculated Euler angles and shift tensor with the experimentally determined EFG at the CCR center of UPMC using an RS/6000 Regatta Power 4 (1.1 GHz) computer. ^{35}Cl spectra were fitted using the *DMFIT* program.[18]

Computational Method

The calculations were performed within Kohn−Sham DFT using the PARATEC code.[19] The PBE generalized gradient approximation[20] was used, and the valence electrons were described by norm-conserving pseudopotentials[21] in the Kleinman−Bylander[22] form. The core definition for O, N, and C is $1s^2$, and it is $1s^22s^22p^6$ for Cl. The core radii are 1.6 au for C, 1.45 au for N, 1.5 au for O, and 1.9 a.u for Cl. The wave functions are expanded on a plane-wave basis set with a kinetic energy cutoff of 80 Ry. The crystalline structure is described as an infinite periodic system using periodic boundary conditions. The NMR calculations were performed for the experimental geometries determined by neutron diffraction for the different amino acids: L-alanine,[23] L-tyrosine hydrochloride,[24] glycine hydrochloride,[25] L-valine hydrochloride,[26] L-alanine hydrochloride,[27] L-tyrosine,[24] and α-glycine.[28] The corresponding structures are presented in Figure 1. ^{17}O calculations on L-glutamic acid hydrochloride have been previously reported by Yates et al.[16]

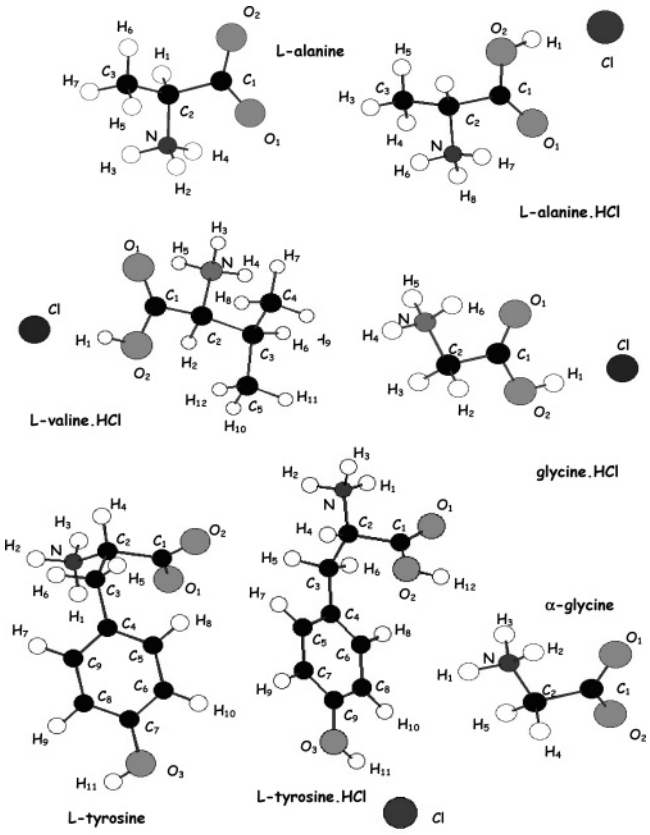

Figure 1. Schematic representation of the amino acids studied: L-alanine, L-tyrosine hydrochloride, glycine hydrochloride, L-valine hydrochloride, L-alanine hydrochloride, L-tyrosine, and α-glycine.

The integrals over the first Brillouin zone are performed using a Monkhorst−Pack 2 × 2 × 2 *k*-point grid[29] for the charge density and electric field gradient calculation and a 4 × 4 × 4 *k*-point grid for the chemical shift tensor calculation. It should be noted that increasing the size of the Monkhorst−Pack grid and the plane-wave cutoff energy level gives practically identical NMR parameters: chemical shift values and quadrupolar coupling constants vary less than 0.1 ppm and 0.01 MHz, respectively. The calculations have been performed at the IDRIS supercomputer center of the CNRS using a parallel IBM Power4 (1.3 GHz) computer: The calculation of the EFG and the CS tensor requires 1 and 2 h, respectively, on 16 processors.

The shielding tensor is computed using the GIPAW[15] approach, which permits the reproduction of the results of a fully converged all-electron calculation, while EFG tensors are computed using a PAW approach. The isotropic chemical shift δ_{iso} is defined as $\delta_{iso} = -[\sigma - \sigma^{ref}]$ where σ is the isotropic shielding (one-third of the trace of the NMR shielding tensor) and σ^{ref} is the isotropic shielding of the same nucleus in a reference system. In our calculations, absolute shielding tensors are obtained. To fix the ^{17}O scale, σ^{ref} was chosen in such a way that the sum of all calculated δ_{iso} for a series of SiO_2 polymorphs coincides with the corresponding sum of experi-

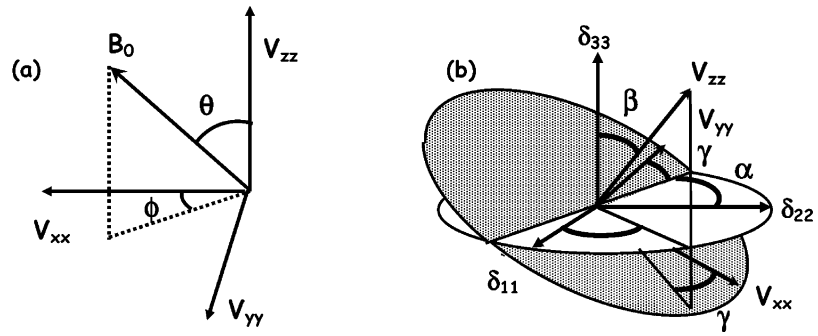

Figure 2. (a) Orientation of the magnetic field B_0 in the quadrupolar PAS. (b) Euler angles relating EFG and CS tensors.

mental values.[30] The resulting σ^{ref} for ^{17}O is 261.5 ppm. Similarly, for ^{13}C, σ^{ref} was fixed so that the average sum of experimental and calculated chemical shifts in phenylphosphonic acid[31] coincide, which leads to $\sigma^{ref}(^{13}C) = 170.9$ ppm. Since few ^{15}N data were available, an external referencing corresponding to solid nitromethane[32] was chosen (($\delta_{iso}(^{15}N) = 0$ ppm) and gives $\sigma^{ref}(^{15}N) = -154.3$ ppm. Similarly, only a few ^{35}Cl spectra have been recorded, so an external reference corresponding to crystalline NaCl[33] was chosen ($\delta_{iso}(^{35}Cl) = 0$ ppm), which gives $\sigma^{ref}(^{35}Cl) = 972.2$ ppm.

Diagonalization of the symmetrical part of the calculated shielding tensor provides its principal components δ_{11}, δ_{22}, and δ_{33} defined as $|\delta_{33} - \delta_{iso}| \geq |\delta_{11} - \delta_{iso}| \geq |\delta_{22} - \delta_{iso}|$ and $\delta_{iso} = {}^1/_3(\delta_{11} + \delta_{22} + \delta_{33})$. Similarly, the principal components V_{xx}, V_{yy}, and V_{zz} of the EFG tensor defined as $|V_{zz}| \geq |V_{xx}| \geq |V_{yy}|$ are obtained by diagonalization of the tensor. The quadrupolar interaction can then be characterized by the quadrupolar coupling constant C_Q, and the asymmetry parameter η_Q defined as

$$C_Q = eQV_{zz}/h \text{ and } \eta_Q = (V_{yy} - V_{xx})/V_{zz}$$

It is worth noticing that the program outputs both tensors in the crystal axis system. Absolute orientation in the molecular frame of the shielding and EFG tensors as well as their relative orientation can therefore be obtained. The relative orientation between the two tensors using three Euler angles (α, β, γ) was therefore extracted from the first-principles calculations. The transformation matrix $R(\alpha, \beta, \gamma)$ was used to deduce the new directional cosines of the CS tensor with respect to the EFG system is written as

$$R(\alpha, \beta, \gamma) = \begin{pmatrix} \cos\gamma\cos\beta\cos\alpha - \sin\gamma\sin\alpha & \cos\gamma\cos\beta\sin\alpha + \sin\gamma\cos\alpha & -\sin\beta\cos\gamma \\ -\sin\gamma\cos\beta\cos\alpha - \cos\gamma\sin\alpha & -\sin\gamma\cos\beta\sin\alpha + \cos\gamma\cos\alpha & \sin\beta\sin\gamma \\ \sin\beta\cos\alpha & \sin\beta\sin\alpha & \cos\beta \end{pmatrix}$$

$$= \begin{pmatrix} R_{11} & R_{21} & R_{31} \\ R_{12} & R_{22} & R_{32} \\ R_{13} & R_{23} & R_{33} \end{pmatrix}$$

In the quadrupolar PAS (principal axis system), the frequency contribution of the CS tensor can be expressed as $\nu_{CS} = -\nu_0(\delta_{11}X'^2 + \delta_{22}Y'^2 + \delta_{33}Z'^2)$ with

$$X' = R_{11}\cos\phi\sin\theta + R_{12}\sin\phi\sin\theta + R_{13}\cos\theta$$
$$Y' = R_{21}\cos\phi\sin\theta + R_{22}\sin\phi\sin\theta + R_{23}\cos\theta$$
$$Z' = R_{31}\cos\phi\sin\theta + R_{32}\sin\phi\sin\theta + R_{33}\cos\theta$$

where θ and ϕ describe the orientation of the static magnetic field B_0 in the quadrupolar PAS (Figure 2a). The Euler angles (α, β, γ) describing the relative orientation of the CS tensors with respect to the EFG systems (Figure 2b) could therefore be extracted.

With our convention, the set of Euler angles (α, β, γ) corresponds to the following input in the *SIMPSON* program:

```
Quadrupole  0  0  0
Shift       α  β  γ
```

Results and Discussion

Experimental Results. *^{17}O NMR Spectra.* Figure 3 shows the experimental ^{17}O MAS and static NMR spectra recorded at 14.1 T of L-alanine and glycine−HCl. For glycine, the MAS spectrum clearly shows two signals, one centered near 300 ppm from the C═O oxygen, the other centered near 150 ppm from the OH oxygen;[5] while the static spectrum is much more difficult to interpret. For L-alanine, even the MAS spectrum shows two overlapping lines, which were resolved and assigned by a combination of double rotation (DOR) and multiple quantum (MQ) experiments by Pike et al.[5] The static spectrum at this field is relatively featureless. The isotropic chemical shift values, quadrupolar coupling constants, and asymmetry parameters extracted from the fit of the MAS spectra for L-alanine, L-valine−HCl, glycine−HCl, and L-tyrosine−HCl are reported in Table 1.

^{35}Cl NMR Spectra. Figure 4 shows the experimental ^{35}Cl MAS and static NMR spectra recorded at 14.1 T of glycine−HCl, L-tyrosine−HCl, L-valine−HCl, and L-glutamic acid−HCl, showing well-defined shapes dominated by second-order qua-

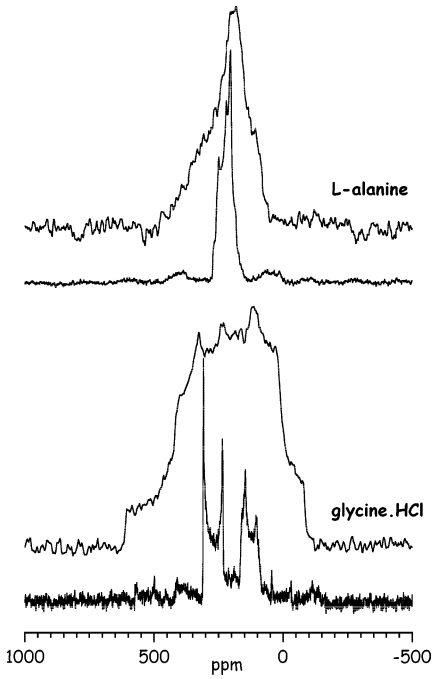

Figure 3. Experimental ^{17}O MAS and static NMR spectra recorded at 14.1 T of L-alanine and glycine−HCl.

TABLE 1: Experimental and Calculated ^{17}O Isotopic Chemical Shift Values, C_Q, and η_Q Parameters for L-Alanine, L-Alanine−HCl, L-Valine−HCl, Glycine−HCl, and L-Tyrosine−HCl

		δ_{iso} (ppm) (±1 ppm)		C_Q (MHz) (±0.1 MHz)		η_Q (±0.1)	
sample	site	exptl	calcd	exptl	calcd	exptl	calcc
L-alanine	O1	284.0	292.3	7.86	8.20	0.28	0.29
	O2	260.5	274.4	6.53	6.90	0.70	0.67
L-alanine−HCl	O1	327.8	322.2	8.31	8.24	0.0	0.05
	O2	176.7	181.9	7.29	7.89	0.20	0.21
L-valine−HCl	O1	351.0	338.7	8.40	8.67	0.03	0.04
	O2	181.0	181.3	7.35	7.68	0.21	0.24
glycine−HCl	O1	333.0	331.2	8.40	8.62	0.0	0.00
	O2	178.0	181.3	7.60	7.77	0.25	0.25
L-tyrosine−HCl	O1	327.0	319.3	8.22	8.47	0.0	0.01
	O2	183.0	185.7	7.35	7.46	0.19	0.20
	O3	83.0	90.5	8.56	8.60	0.65	0.8

drupolar interaction, characteristic of intermediate asymmetry parameters. The isotropic chemical shift values, quadrupolar coupling constants, and asymmetry parameters extracted from the fit of these spectra are reported in Table 2. The parameters obtained for L-tyrosine− HCl are consistent with those previously reported.[14] The variation in chemical shifts for the different compounds appears relatively small (less than 12 ppm) compared to the total known chemical shift range for chlorine, 1500 ppm,[34] as already observed for other organic hydrochlorides.[14]

First-Principles Calculations. *^{13}C CS Tensor.* One of the benefits of the calculation is that the NMR parameters of all the nuclei present in the structure are determined simultaneously. Although the ^{17}O experimental data available for amino acids are somewhat limited, ^{13}C chemical shift tensor components have been experimentally measured for all of them.[35] As an initial check of the validity of our approach, the values for L-alanine, L-tyrosine, and α-glycine are indicated in Table 3 and compared with those obtained by the calculations. There is an excellent agreement between our δ_{ii} and δ_{iso} calculated values and the experimental data for all carbon sites, the correlations exhibiting slopes of 1.02 ($R = 0.99$) and 1.00 ($R = 0.99$),

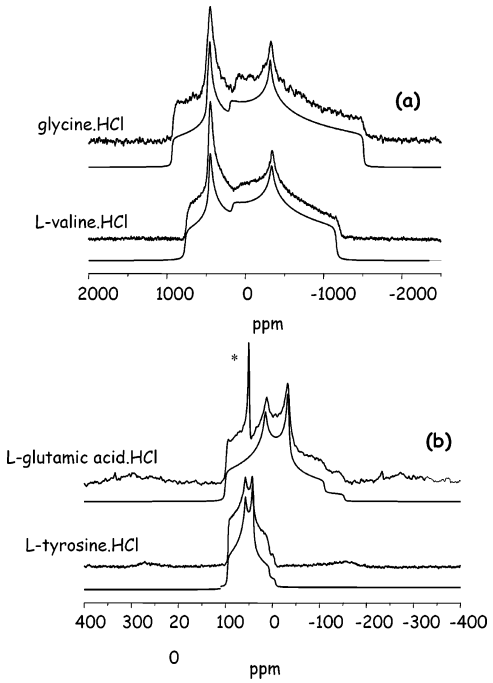

Figure 4. ^{35}Cl NMR experimental and fitted[18] (a) static spectra of glycine−HCl and L-valine−HCl and (b) MAS spectra of L-glutamic acid−HCl and L-tyrosine−HCl (*additionnal signal due to an unknown impurity).

TABLE 2: Experimental and Calculated ^{35}Cl Isotopic Chemical Shift Values, C_Q and η_Q Parameters for L-Tyrosine−HCl, Glycine−HCl, L-Valine−HCl, L-Alanine−HCl, and L-Glutamic Acid−HCl[a]

	δ_{iso} (±1 ppm)		C_Q (±0.1 MHz)		η_Q (±0.1)	
sample	exptl	calcc	exptl	calcd	exptl	calcd
L-tyro−HCl	95	97	2.3	3.3	0.7	0.48
gly−HCl	117	108	6.5	8.46	0.6	0.81
L-val−HCl	114	105	6.0	8.14	0.5	0.54
L-ala−HCl		99		8.42		0.60
L-glu−HCl*	104	99	3.7	5.26	0.6	0.6

[a] *L-Glutamic acid−HCl calculated by J. R. Yates et al.[16]

TABLE 3: Experimental[35] and Calculated ^{13}C Chemical Shift Tensor Components for L-Alanine, α-Glycine, and L-Tyrosine[a]

		δ_{iso} (ppm)		δ_{11} (ppm)		δ_{22} (ppm)		δ_{33} (ppm)	
sample	site	exptl	calcd	exptl	calcd	exptl	calcd	exptl	calcd
L-alanine	C1	176.8	178	239	244	184	184	106	105
	C2	50	49.2	63	66	56	55	30	26
	C3	19.8	13.7	31	26	19	15	7	1
α-glycine	C1	176.2	174.9	246	247	179	179	106	100
	C2	43.5	39.6	61	58	46	42	24	19
L-tyrosine	C1	175.8	175.3	238	240	184	180	106	103
	C2	56.7	56.2	67	70	56	61	48	38
	C3	37	35.2	51	43	38	39	21	23
	C4	123.9	125.5	222	225	137	138	13	12
	C5−9	131	133.5	212	217	144	148	38	45
	C6−8	118.3	117.4	179	186	143	141	27	21
	C7	155.8	159.0	245	238	156	169	66	70

[a] $\delta_{iso} = {}^1/_3(\delta_{11} + \delta_{22} + \delta_{33})$; $|\delta_{33} - \delta_{iso}| \geq |\delta_{11} - \delta_{iso}| \geq |\delta_{22} - \delta_{iso}|$.

respectively, as shown in Figure 5. The precision obtained for the shielding tensors is comparable to that recently reported for L-alanine and α-glycine by Grant et al.[36] using an embedded ion method and is slightly better than the results obtained for the carboxyl carbon atoms in L-alanine and α-glycine using an

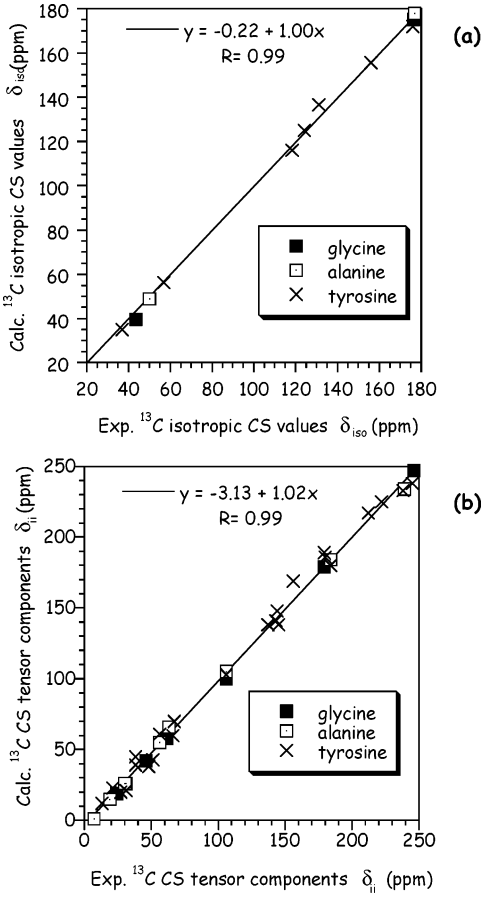

Figure 5. Comparison between experimental and calculated ^{13}C isotropic chemical shift values (a) and CS tensor components (δ_{ii}) (b) for L-alanine, L-tyrosine, and α-glycine.

ONIOM method calculation.[37] The absolute orientation in the molecular frame of the ^{13}C CS tensors is also given for each of the carbon sites. It is interesting to notice that the tensor components δ_{11} and δ_{22} of the carboxyl C_1 atom are included in the plane defined by both $C_1{=}O_1$ and $C_1{-}O_2$ bonds (Figure 6). Moreover, δ_{11} lies approximately along the bisector of the O−C−O angle as already reported for glycine.[38]

Nitrogen EFG and CS Tensors. ^{14}N EFG tensor components have been experimentally measured for α-glycine[38−40] and L-alanine,[41,40] and the corresponding C_Q and η_Q values are reported in the top section of Table 4 with the corresponding calculated values (using the experimental value[42] of the quadrupole moment $Q = 2.04 \times 10^{-30}$ m^2). There is a good agreement between experiment and calculation, with the values being within ∼0.1 MHz. The accuracy obtained is somewhat better, particularly for the asymmetry parameter, than the calculations that used the cluster approach.[40] The absolute orientation in the molecular frame of the EFG tensors calculated for L-alanine and L-tyrosine is presented in Figure 7. It shows that, in both cases, the largest component V_{zz} lies nearly along the C−N bond, while the smallest component V_{yy} is almost perpendicular to the NCC plane, as already experimentally observed for α-glycine.[38]

The ^{15}N chemical shift tensor components have, to our knowledge, only been measured for α-glycine.[36] They are reported in the bottom section of Table 4 together with the experimental isotropic shift for L-alanine[40] and the calculated tensor values for α-glycine, L-alanine, and L-tyrosine. There is a satisfying agreement between experimental and calculated

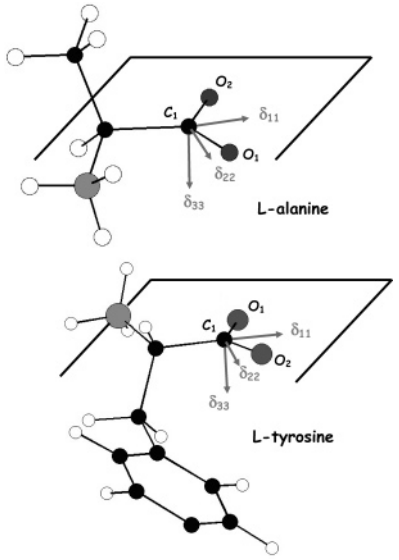

Figure 6. Calculated orientations of the ^{13}C CS tensors of the C_1 atom in the molecular frame of L-alanine, and L-tyrosine.

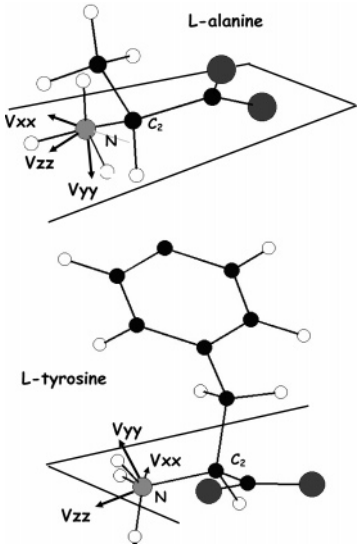

Figure 7. Calculated orientations of the ^{14}N EFG tensors of the N atom in the molecular frame of L-alanine, and L-tyrosine.

values for α-glycine and the isotropic shift for L-alanine, but comparison with other experimental data would be useful to determine the accuracy of the calculations.

^{17}O CS and EFG Tensors. The calculated values of the isotropic chemical shift, quadrupolar coupling constant (using the experimental value[42] of the quadrupole moment $Q = 2.55 \times 10^{-30}$ m^2), and asymmetry parameter are reported in Table 1 together with the experimental values. To the best of our knowledge, ^{17}O calculations using the cluster approach have not been reported on these amino acids. The correlation between the calculated and experimental ^{17}O isotropic chemical shift values is good with a slope of 0.95 ($R = 0.99$) as shown in Figure 8a. While the calculations reproduce the experimental ^{17}O C_Q values within 0.5 MHz and give good agreement for η, they systematically slightly overestimate C_Q values (Figure 8b) by about 4% as already observed[30,43] for ^{17}O. To obtain information about the ^{17}O CS and EFG tensors, static experiments were carried out at two different magnetic fields, 8.4 and 14.1 T, on L-alanine, glycine−HCl, and L-valine−HCl. Figure 9 shows the corresponding experimental spectra exhibiting numerous discontinuities that are difficult to interpret. It is very

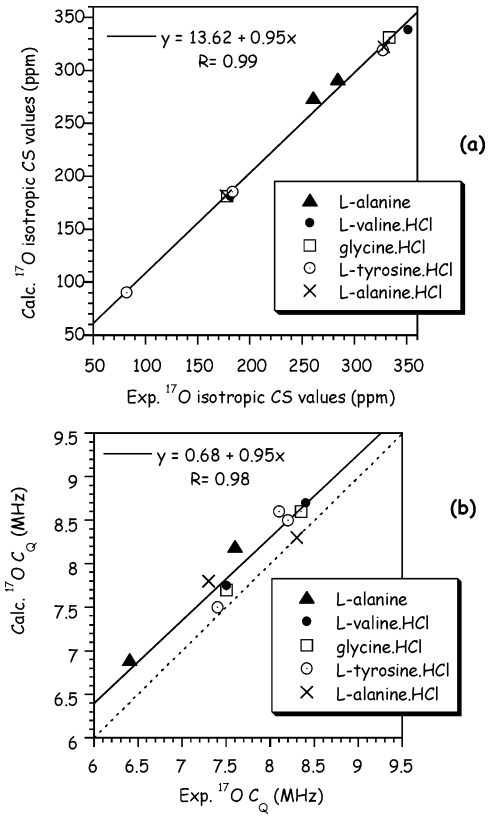

Figure 8. Comparison between experimental and calculated ^{17}O isotropic chemical shift values (a) and ^{17}O quadrupolar coupling constants (b) for the different oxygen sites in L-alanine, glycine−HCl, L-tyrosine−HCl, L-alanine−HCl, and L-valine−HCl.

difficult to determine five unknowns (extent of the CS tensor and relative orientation between CS and EFG tensor) from analyzing static spectra for multisite samples, even at two magnetic fields. Single-crystal NMR experiment would be the best technique to precisely determine the tensors, but large single crystals, especially ^{17}O-labeled ones, are difficult to obtain. Combining calculations with experimental data appears to be an efficient and elegant way to establish the orientation of the ^{17}O EFG and CS tensors[1] and helps to confirm the assignment.

The calculated Euler angles (α, β, γ) describing the relative orientation of the CS tensors with respect to the EFG systems for the different oxygen sites as well as the corresponding δ_{ii} values are reported in Table 5. The calculated spectra using these parameters (Figure 9) show a very satisfying agreement at both fields with experimental data. Moreover, absolute orientation in the molecular frame (Figure 10) of the ^{17}O CS and EFG tensors can be calculated for each of the oxygen sites. Contrary to what was observed previously for the CS tensor of the C_1 carbon atoms, none of the ^{17}O tensor components appear in the plane defined by both $C_1{=}O_1$ and $C_1{-}O_2$ bonds. It can nonetheless be noticed that the V_{xx} component of the O_1 EFG tensor is approximately aligned with the $C_1{=}O_1$ bond.

TABLE 5: Calculated ^{17}O CS Tensors and Relative Orientation with EFG Tensors for L-Alanine, L-Alanine−HCl, L-Valine−HCl, Glycine−HCl, L-Tyrosine−HCl, L-Tyrosine, and α-Glycine

sample	site	δ_{iso} (ppm)	δ_{11} (ppm)	δ_{22} (ppm)	δ_{33} (ppm)	α (°)	β (°)	γ (°)
L-alanine	O1	292.3	507.7	368.2	3.0	40	−90	95
	O2	274.4	449.3	314.0	60	−30	−95	−95
L-alanine−HCl	O1	322.2	559.3	435.8	−27.9	−20	115	−70
	O2	181.9	84.4	127	334.5	−65	85	−175
L-val−HCl	O1	338.7	592.9	454.9	−31.8	60	90	10
	O2	188.5	54.1	82.9	428.5	80	55	−100
glycine-HCl	O1	333.0	589	431	−32	55	90	40
	O2	178.0	84	107	343	85	−105	−80
L-tyro−HCl	O1	319.3	552.9	443.4	−37.5	150	−90	80
	O2	185.7	78.9	131.1	347.2	−90	−115	175
	O3	90.5	131.4	85.4	54.7	−89	108	103
L−tyrosine	O1	294.8	518.5	353.4	12.1	140	−90	95
	O2	273.5	452.1	312.2	56.3	−150	−90	85
	O3	85.0	142.9	80.3	31.8	75	110	−85
α−glycine	O1	297.6	507.7	340.5	44.5	35	−90	−90
	O2	282.6	471.5	341.5	34.9	40	−90	90

Impact of Crystallographic Data on the ^{17}O Calculations. L-Alanine has had its structure determined by both neutron[23] and X-ray[44] diffraction, and calculations for both structures were performed to determine the sensitivity of the calculated NMR parameters to small variations in the structure.

The corresponding ^{13}C, ^{15}N, and ^{17}O NMR parameters are summarized and compared with experimental data in Table 6. The calculated ^{13}C and ^{15}N isotropic chemical shift values are relatively insensitive to structure and close to experiment in both cases, being slightly better with the X-ray structure, while the shift tensor components are also similar. The calculated ^{17}O C_Q and η_Q values do not change much between the structures, with a very good agreement for η_Q and an overestimation for C_Q as discussed previously. The main differences concern the ^{17}O chemical shift values. Examination of the shift tensor (Table 6) shows that all components of the CS are larger with the X-ray structure; the calculation with the neutron structure gives an isotropic shift about 10 ppm too high compared with experiment, and this difference is significantly larger when the X-ray structure is being used around 18 ppm. Bond distances and hydrogen bond lengths in both structures are reported in Table 7. The main differences in the structure concern the C−H and N−H bond lengths as well as the hydrogen bonding distances. This strongly suggests that the calculated ^{17}O isotropic chemical shift values are very sensitive to the proton position in these

TABLE 4: Nitrogen NMR Parameters for L-Alanine, α-Glycine, and L-Tyrosine

Experimental[38,40] and Calculated ^{14}N C_Q and η_Q Values

	C_Q (MHz)			η_Q		
sample	exptl		calcd	exptl		calcd
α-glycine	1.17[40]	1.18[38]	1.28	0.51[40]	0.54[38]	0.53
L-alanine	1.14[40]	1.20[38]	1.25	0.24[40]	0.26[38]	0.26
L-tyrosine			1.10			0.36

Experimental (α-glycine[36] and L-alanine[40]) and Calculated ^{15}N Chemical Shift Tensor Components

	δ_{iso} (ppm)		δ_{11} (ppm)		δ_{22} (ppm)		δ_{33} (ppm)	
sample	exptl	calcd	exptl	calcd	exptl	calcd	exptl	calcd
α-glycine	−346.3	−345.3	−337.6	−330.5	−346.0	−350.1	−355.4	−355.2
L-alanine	−337.1	−340.1		−329.3		−340.5		−350.4
L-tyrosine		−342.9		−328.6		−339.9		−360.3

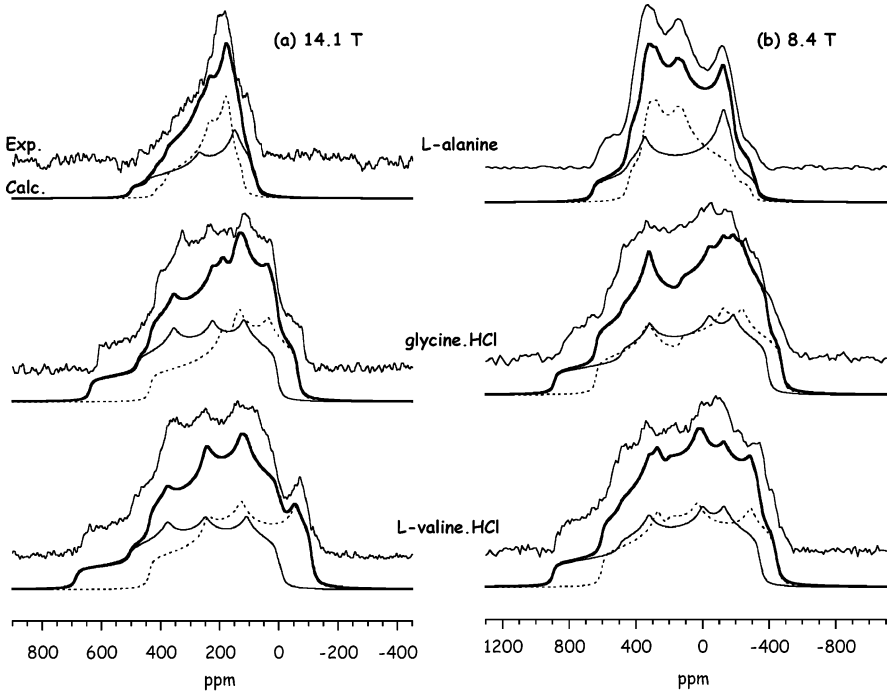

34

Figure 9. Experimental and calculated[17] ^{17}O static NMR spectra for L-alanine, glycine−HCl, and L-valine−HCl recorded at (a) 14.1 T and (b) 8.4 T. The calculated O_1 line is plain, the calculated O_2 line is dashed, and the global calculated spectrum is indicated in a bold plain line.

TABLE 6: Experimental and Calculated ^{13}C, ^{15}N, and ^{17}O Isotropic Chemical Shift Values, Chemical Shift Tensor Components, as well as ^{17}O Quadrupolar Parameters in L-Alanine[a]

	δ_{iso} (ppm)			δ_{11} (ppm)		δ_{22} (ppm)		δ_{33} (ppm)	
	exptl	calcd (a)	calcd (b)	calcd (a)	calcd (b)	calcd (a)	calcd (b)	calcd (a)	calcd (b)
C1	176.8	178.0	181.1	244	246.7	184	189.8	105	106.7
C2	50.0	49.0	51.6	66	67	55	58	26	29.5
C3	19.8	13.7	17.4	26	30	15	16.7	1	5
N	−337.1	−340.1	−336.2	−329.3	−324.1	−340.5	−336.6	−350.4	−347.8

	δ_{iso} (ppm)			C_Q			η_Q		
	exptl	calcd (a)	calcd (b)	exptl	calcd (a)	calcd (b)	exptl	calcd (a)	calcd (b)
O1	284.0	292.3	300.6	7.86	8.20	8.48	0.28	0.29	0.31
O2	260.5	274.4	280.9	6.53	6.90	6.83	0.70	0.67	0.73

	δ_{11} (ppm)		δ_{22} (ppm)		δ_{33} (ppm)	
	calcd (a)	calcd (b)	calcd (a)	calcd (b)	calcd (a)	calcd (b)
O1	507.7	515.6	368.2	380.6	3.0	5.6
O2	449.3	457.4	314.0	322.6	60	62.8

[a] Calculations are performed using both neutron diffraction (a)[23] and X-ray[44] (b) structures for L-alanine.

TABLE 7: Bond Distances (Å) in L-Alanine

	C1−O1	C1−O2	C1−C2	C2−N	C2−C3	N−H1	N−H2	N−H3
X-ray[44]	1.248	1.267	1.535	1.488	1.526	1.044	1.018	1.082
neutron[23]	1.242	1.258	1.531	1.487	1.524	1.029	1.031	1.047
difference	0.006	0.009	0.004	0.001	0.002	0.015	−0.013	0.035

	C2−H4	C3−H5	C3−H6	C3−H7	O1···H2−N	O2···H3−N	O2···H4−N
X-ray[44]	1.125	1.086	1.118	1.082	1.827	1.722	1.832
neutron[23]	1.093	1.081	1.082	1.081	1.861	1.78	1.828
difference	0.032	0.005	0.036	0.001	−0.034	−0.058	0.004

samples. It should however be noticed that a strong linear correlation of the ^{17}O isotropic chemical shift values with the C═O bond length exhibiting a slope of ∼−1200 ppm/Å was experimentally observed for amino acids.[5] The small difference in the C═O bond lengths between both structures could therefore also induce a significant change in the corresponding δ_{iso} values. The positions of the proton in the X-ray structure were relaxed using DFT, which changed the chemical shift by less than 1 ppm.

Hydrogen-Bonding Effect. Hydrogen-bonding interactions in the different amino acids studied are reported in Table 8, while the corresponding ^{17}O chemical shift parameters are summarized in Tables 5 and 6. Obviously, the C═O_1···H hydrogen bond lengths are longer in the hydrochloride samples,

TABLE 8: Summary of Crystal Structure Data Including O···H Hydrogen Bonding in the Amino Acids Studied

compound	crystal form	space group	site	hydrogen bonding	ref
L-alanine	orthorombic	$P2_12_12_1$	O1	$O_1\cdots H_2-N$ (1.861 Å)	23
			O2	$O_2\cdots H_3-N$ (1.780 Å)	
				$O_2\cdots H_4-N$ (1.828 Å)	
L-tyrosine	orthorombic	$P2_12_12_1$	O1	$O_1\cdots H_{11}-O_2$ (1.689 Å)	24
			O2	$O_2\cdots H_3-N$ (1.853 Å)	
α-glycine	monoclinic	$P2_1/n$	O1	$O_1\cdots H_1-N$ (1.728 Å)	28
			O2	$O_2\cdots H_2-N$ (1.832 Å)	
glycine−HCl	monoclinic	$P2_1/c$	O1	$O_1\cdots H_6-N$ (2.222 Å)	25
L-valine−HCl	monoclinic	$P2_1$	O1	$O_1\cdots H_3-N$ (2.455 Å)	26
L-alanine−HCl	orthorombic	$P2_12_12_1$	O1	$O_1\cdots H_7-N$ (2.078 Å)	27
L-tyrosine−HCl	monoclinic	$P2_1$	O1	$O_1\cdots H_2-N$ (2.420 Å)	24
			O3	$O_3\cdots H_{12}-O_2$ (1.609 Å)	

while the isotropic chemical shift values are higher. More precisely, it seems that there are correlations between the C═O_1···H bond length and tensor components (Figure 11): δ_{11}, δ_{22}, and δ_{iso} increase linearly, while δ_{33} decreases linearly with the C═O···H—N hydrogen bond length. Such a tendency showing an increase of the δ_{33} with the hydrogen bond strength has already been observed for C═O···H—N[1] and C—O···H—O[2] hydrogen bonds. The dependence of all CS tensor components on the hydrogen bond distance r(O···N) has also been reported for the carbonyl tensors in amides[1] where the three CS tensor components changed linearly with r(O···N).

^{35}Cl CS and EFG Tensors. The calculated isotropic chemical shift values, quadrupolar coupling constants, and asymmetry parameters are reported in Table 2, while the calculated CS tensors and relative orientation with EFG tensors for glycine−HCl, L-tyrosine−HCl, L-valine−HCl, and L-alanine−HCl are reported in Table 9. The span of the CS tensor $\Omega = |\delta_{11}-\delta_{33}|$ is between 78 and 157 ppm, with the calculated value of 91 ppm for L-tyrosine−HCl being consistent with previously reported values.[14] It should be noticed that the calculated C_Q values reported in Table 2 are systematically overestimated by

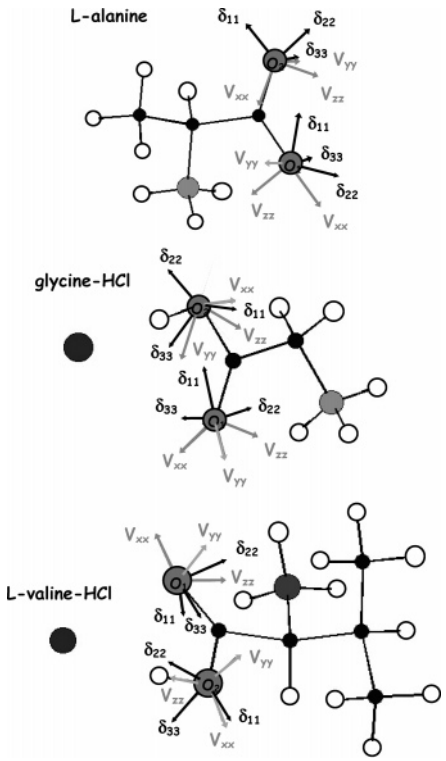

Figure 10. Calculated orientations of the ^{17}O CS tensors (δ_{ii}) and EFG tensors (V_{ii}) in the molecular frame of L-alanine, glycine−HCl, and L-valine−HCl.

TABLE 9: Calculated ^{35}Cl CS Tensors and Relative Orientation with EFG Tensors for Glycine−HCl, L-Tyrosine−HCl, L-Valine−HCl, and L-Alanine−HCl

sample	δ_{iso} (ppm)	δ_{11} (ppm)	δ_{22} (ppm)	δ_{33} (ppm)	α (°)	β (°)	γ (°)
L-tyro−HCl	97	57	87	148	40	75	35
gly−HCl	108	162	114	48	−45	5	40
L-val−HCl	105	181	107	27	−20	−175	180
L-ala−HCl	99	61	97	139	10	90	−15

TABLE 10: ^{35}Cl Experimental[9] and Calculated Nuclear Quadrupole Frequency of Various Carbon−Chlorine Compounds[45−47]

		^{35}Cl nuclear quadrupole frequency	
sample	site	calcd	exptl[9]
O═CCl_2[45]	Cl #1	33.49	36.23
	Cl #2	33.82	
p·$(OH)_2C_6Cl_4$[46]	Cl #1	35.27	36.74
	Cl #2	35.61	36.96
p·$O_2C_6Cl_4$[47]	Cl #1	35.64	36.79
	Cl #2	36.17	36.86

∼20%. In an effort to determine the cause of this discrepancy, the EFG of some covalently bonded chlorine in organic compounds (observed by NQR[9]) was calculated. The values (Table 10) were found to be in satisfying agreement with experiment (i.e., within ∼4% in most cases). Thus, the difference in C_Q for the amino acids is possibly due to H or mobility effects of the anion that are not taken into account in the calculations.

Hydrogen-Bonding Effect. The experimental values of C_Q are very similar (∼6.3 MHz) for glycine−HCl, L-alanine−HCl, and L-valine−HCl and are almost three times bigger than that observed for L-tyrosine−HCl (2.3 MHz). L-Glutamic acid−HCl exhibits an intermediate value (3.7 MHz). Previously reported studies indicate the impact of the length of the Cl···H contacts on the C_Q values,[10,14] and the same approach was adopted for a better understanding of the ^{35}Cl spectra. The Cl···H bond lengths in the different amino acids are reported in Table 11 and show the presence of one short Cl···H—O contact (2 Å) and two relatively short Cl···H—N contacts (<2.3 Å) in glycine−HCl, L-alanine−HCl, L-valine−HCl, and L-glutamic acid−HCl, while a Cl···H—O short contact (2 Å) and only one

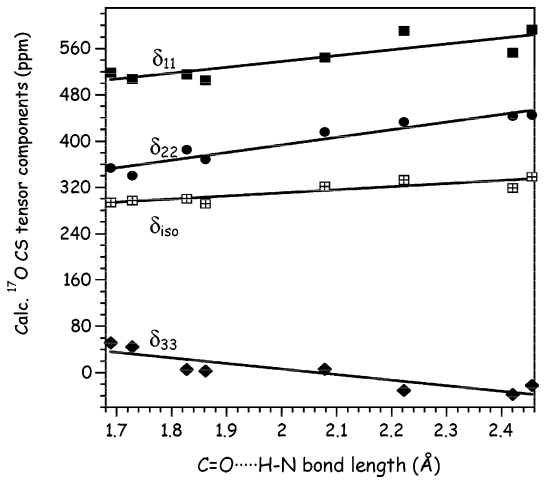

Figure 11. Calculated ^{17}O CS tensor components vs C═O···H—N hydrogen bond length (in Å) for amino acids studied. Results for both structural determinations (X-ray and neutron diffraction) for alanine are shown. Equations of the linear correlations: δ_{iso} ($y = 203.9 + 53.2x$; $R = 0.89$), δ_{11} ($y = 336.3 + 100.6x$; $R = 0.86$), δ_{22} ($y = 130.2 + 131.6x$; $R = 0.96$), δ_{33} ($y = 198.1 - 96.0x$; $R = 0.89$).

TABLE 11: Cl···H Hydrogen Bonding in the Studied Hydrochloride Amino Acids

compound	hydrogen bonding	ref
glycine−HCl	Cl···H_1−O_2 (2.008 Å)	25
	Cl···H_4−N (2.123 Å)	
	Cl···H_5−N (2.159 Å)	
	Cl···H_6−N (2.592 Å)	
	Cl···H_3−C_2 (2.661 Å)	
L-tyrosine−HCl	Cl···H_{11}−O_3 (2.077 Å)	24
	Cl···H_1−N (2.378 Å)	
	Cl···H_2−N (2.471 Å)	
	Cl···H_3−N (2.505 Å)	
	Cl···H_5−C_3 (2.661 Å)	
L-valine−HCl	Cl···H_1−O_2 (1.989 Å)	26
	Cl···H_4−N (2.159 Å)	
	Cl···H_5−N (2.263 Å)	
	Cl···H_3−N (2.355 Å)	
	Cl···H_6−C_3 (2.875 Å)	
	Cl···H_7−C_4 (2.875 Å)	
L-alanine−HCl	Cl···H_1−O_2 (2.042 Å)	27
	Cl···H_6−N (2.205 Å)	
	Cl···H_8−N (2.226 Å)	
	Cl···H_7−N (2.732 Å)	
l-glutamic acid	Cl···H_2−O_4 (2.073 Å)	
	Cl···H_4−N (2.107 Å)	
	Cl···H_5−N (2.137 Å)	
	Cl···H_{10}−C_4 (3.005 Å)	

relatively short Cl···H−N contact (<2.3 Å) is present in L-tyrosine−HCl, as illustrated in Figure 12. ^{35}Cl spectra appear therefore as a good probe of the hydrogen-bonding environment, with the C_Q value seeming to increase with the number of short Cl···H contacts. This assumption is reinforced by analyzing more precisely the case of L-glutamic acid−HCl. The observed C_Q value is indeed smaller than in glycine−HCl, L-alanine−HCl, and L-valine−HCl; and it can be noted in these three samples that a fourth intermediately short Cl···H−N contact (<2.8 Å) is present, while it does not appear in L-glutamic acid−HCl (Table 11).

Conclusion

The first-principles calculations presented in this article show that this method reproduces with accuracy all experimental NMR parameters (chemical shift value, chemical shift anisotropy, quadrupolar coupling constant, and asymmetry parameter) on all the nuclei present (i.e., ^{13}C, ^{14}N, ^{15}N, ^{17}O, and ^{35}Cl) and appears therefore as a very powerful tool to assign all kinds of NMR spectra in small biomolecules.

As previously observed in other biomolecules, the ^{17}O NMR chemical shift tensors of amino acids appear to be very sensitive to the local intermolecular hydrogen-bonding interactions: δ_{11}, δ_{22}, and δ_{iso} values increase linearly, while δ_{33} decreases linearly with the C═O···H−N hydrogen bond lengths. The different δ_{ii} values as well as the relative orientation of the ^{17}O EFG and CS tensors were obtained from first-principles calculations, and the resulting calculated ^{17}O static spectra at two different fields show an excellent agreement with experimental data. Since the calculation method used gives the NMR parameters of all nuclei present, ^{13}C, ^{14,15}N, and ^{35}Cl NMR values could also be compared with experimental values and exhibit a very satisfactory agreement as well. The influence of the Cl···H hydrogen bonding on the ^{35}Cl C_Q values could also be investigated and shows a consistent increase of the chlorine quadrupolar coupling constants with the number of short Cl···H contacts.

The importance of the hydrogen bonding on the NMR parameters was emphasized by investigating the impact of the crystallographic data on the ^{17}O calculations. Calculated δ_{iso} values appear to be very sensitive to the proton position in these samples, with a better agreement with experimental data being obtained for structures determined by neutron diffraction. This suggests that the limiting factor in the calculations may be the accuracy of the structure.

This study confirms the usefulness of ^{17}O and ^{35}Cl solid-state NMR experiments in studying hydrogen bonding in biological systems. Combining experimental data with first-principles calculations is a very efficient and elegant way to extract the full CS and EFG tensors in these systems and to determine the sensitivity of the NMR parameters to the bonding state.

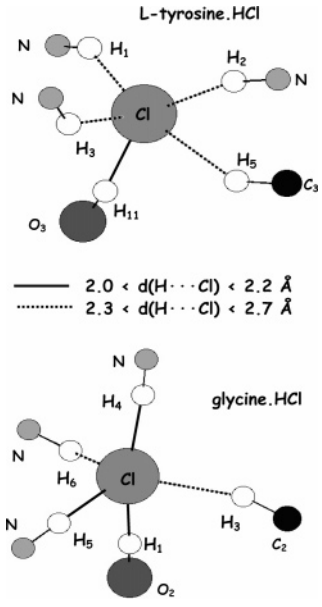

Figure 12. Schematic representation of H···Cl contacts for glycine−HCl and L-tyrosine−HCl. Short contacts ($2.0 < d(H\cdots Cl) < 2.2$ Å) are indicated with plain lines, while longer contacts ($2.3 < d(H\cdots Cl) < 2.7$ Å) are indicated with dashed lines.

Acknowledgment. We wish to thank Dr. A. Kukol, V. Lemaitre, and Prof. A. Watts for ^{17}O enriching the glycine and alanine samples and EPSRC for support. We also thank M. Krawczyk for his help at the CCR center of UPMC. The calculations have been performed on the IDRIS supercomputer center of the CNRS (project 51461).

References and Notes

(1) Yamada, K.; Dong, S.; Wu, G. *J. Am. Chem. Soc.* **2000**, *122*, 11602.
(2) Wu, G.; Dong, S.; Ida, R.; Reen, N. *J. Am. Chem. Soc.* **2002**, *124*, 1768.
(3) Wu, G.; Yamada, K. *Solid State NMR* **2003**, *24*, 196.
(4) Lemaitre, V.; Pike, K. J.; Watts, A.; Anupõld, T.; Samoson, A.; Smith, M. E.; Dupree, R. *Chem. Phys. Lett.* **2003**, *371*, 91.
(5) Pike, K. J.; Lemaitre, V.; Kukol, A.; Anupõld, T.; Samoson, A.; Howes, A. P.; Watts, A.; Smith, M. E.; Dupree, R. *J. Phys. Chem. B* **2004**, *108*, 9256.
(6) Weeding, T. L.; Veeman, W. S. *J. Chem. Soc., Chem. Commun.* **1989**, 946.
(7) Hayashi, S.; Hayamizu, K. *Bull. Chem. Soc. Jpn.* **1990**, *63*, 913.
(8) Skibsted, J.; Jakobsen, H. J. *Inorg. Chem.* **1999**, *38*, 1806.
(9) Lucken, E. A. *Nuclear Quadrupole Coupling Constants*; Academic Press: London, 1969.
(10) Azaïs, T.; Bonhomme, C.; Smith, M. E. *Solid State NMR* **2003**, *23*, 14.
(11) Seliger, J.; Zagar, V.; Blinc, R.; Arend, H.; Chapuis, G. *J. Chem. Phys.* **1982**, *78*, 2661.
(12) Blinc, R.; Mali, M.; Osredkar, R.; Seliger, J. *J. Chem. Phys.* **1975**, *63*, 35.
(13) Yesinowski, J. P.; Buess, M. L.; Garroway, A. N.; Ziegerweid, M.; Pines, A. *Anal. Chem.* **1995**, *67*, 2256.

(14) Bryce, D. L.; Gee, M.; Wasylishen, R. E. *J. Phys. Chem. A* **2001**, *105*, 10413.
(15) Pickard, C. J.; Mauri, F. *Phys. Rev. B* **2001**, *63*, 245101.
(16) Yates, J. R.; Pickard, C. J.; Payne, M. C.; Dupree, R.; Profeta, M.; Mauri, F. *J. Phys. Chem. A* **2004**, *108*, 6032.
(17) Bak, M.; Rasmussen, J. T.; Nielsen, N. C. *J. Magn. Reson.* **2000**, *147*, 296 (SIMPSON-http://nmr.imsb.au.dk).
(18) Massiot, D.; Fayon, F.; Capron, M.; King, I.; Le Calvé, S.; Alonso, B.; Durand, J.; Bujoli, B.; Ghan, Z.; Hoatson, G. *Magn. Reson. Chem.* **2002**, *20*, 70.
(19) Pfrommer, B.; Raczkowski, D.; Canning, A.; Louie, S. G. (with contributions from Mauri, F.; Cote, M.; Yoon, Y.; Pickard C.; Heynes, P.) PARATEC (PARAllel Total Energy Code); Lawrence Berkeley National Laboratory, www.nersc.gov/projects/paratec.
(20) Perdew, J. P.; Trucks, G. W.; Keith, T. A.; Frisch, M. J. *J. Chem. Phys.* **1996**, *104*, 14.
(21) Troulier, N.; Martins, J. L. *Phys. Rev. B* **1991**, *43*, 1993.
(22) Kleinman, L.; Bylander, D. *Phys. Rev. Lett.* **1982**, *48*, 1425.
(23) Lehmann, M. S.; Koetzle, T. F.; Hamilton, W. C. *J. Am. Chem. Soc.* **1972**, *94*, 2657.
(24) Frey, M. N.; Koetzle, T. F.; Lehmann, M. S.; Hamilton, W. C. *J. Chem. Phys.* **1973**, *58*, 2547.
(25) Al-Karaghouli, A. R.; Cole, F. E.; Lehmann, M. S.; Miskell, C. F.; Verbist J. J.; Koetzle, T. F. *J. Chem. Phys.* **1975**, *63*, 1360.
(26) Koetzle, T. F.; Golic, L.; Lehmann, M. S.; Verbist, J. J.; Hamilton, W. C. *J. Chem. Phys.* **1974**, *60*, 4690.
(27) Di Blasio, B.; Pavone, V.; Pedone, C. *Cryst. Struct. Commun.* **1977**, *6*, 745.
(28) Jönsson, P.; Kvick, A. *Acta Crystallogr.* **1972**, *B28*, 1827.
(29) Monkhorst, H. J.; Pack, J. D. *Phys. Rev. B* **1976**, *13*, 5188.
(30) Profeta, M.; Mauri, F.; Pickard, C. J. *J. Am. Chem. Soc.* **2003**, *125*, 541.
(31) Gervais, C.; Profeta, M.; Lafond, V.; Bonhomme, C.; Azais, T.; Mutin, H.; Pickard, C. J.; Mauri, F.; Babonneau, F. *Magn. Reson. Chem.* **2004**, *42*, 445.
(32) Trevino, S. F.; Prince, E.; Hubbard, C. R. *J. Chem. Phys.* **1980**, *73*, 2996.
(33) Bragg, W. L. *Nature (London)* **1912**, *90*, 410.
(34) Akitt, J. W. *Multinuclear NMR*; Mason, J., Ed.; Plenum: New York, 1987; Chapter 17.
(35) Ye, C.; Fu, R.; Hu, J.; Hou, L.; Ding, S. *Magn. Reson. Chem*. **1993**, *31*, 699.
(36) Strohmeier, M.; Stueber, D.; Grant, D. M. *J. Phys. Chem. A* **2003**, *107*, 7629.
(37) Zheng, A.; Yang, M.; Yue, Y.; Ye, C.; Deng, F. *Chem. Phys. Lett.* **2004**, *399*, 172.
(38) Haberkorn, R. A.; Stark, R. E.; van Willigen, H.; Griffin, R. G. *J. Am. Chem. Soc.* **1981**, *103*, 2534.
(39) Andersson, L. O.; Gourdji, M.; Guibe, L.; Proctor, W. G. *C. R. Acad. Sci., Paris, Ser. B* **1968,** *267B*, 803.
(40) Giavani, T.; Bildsoe, H.; Skibsted, J.; Jakobsen, H. J. *J. Magn. Res*. **2004**, *166*, 262.
(41) Naito, A.; Ganapathy, S.; Akasaka, K.; McDowell, C. A. *J. Chem. Phys.* **1981**, *76*, 3190.
(42) Pyykkö, P. *Mol. Phys.* **2001**, *99*, 1617.
(43) Charpentier, T.; Ispas, S.; Profeta, M.; Mauri, F.; Pickard, C. J. *J. Phys. Chem. B* **2004**; *108*, 4147.
(44) Destro, R.; Marsh, R. E.; Bianchi, R. *J. Phys. Chem.* **1988**, *92*, 966.
(45) Zaslow, B.; Atoji, M.; Lipscomb, W. N. *Acta Crystallogr*. **1952**, *5*, 833
(46) Sikka, S. K.; Chidambaram, R. *Acta Crystallogr*. **1967**, *23*, 107.
(47) Van Weperen, K. J.; Visser, G. J. *Acta Crystallogr*. **1972**, *B28*, 338.